

RESEARCH

Open Access

Multivariate empirical mode decomposition based sub-frequency bands analysis of the default mode network: a resting-state fMRI data study

Tao Zhang¹, Peng Xu^{1,2*}, Lanjin Guo¹, Rui Chen¹, Rui Zhang¹, Hui He¹, Qiankun Xie¹, Tiejun Liu^{1,2}, Cheng Luo^{1,2} and Dezhong Yao^{1,2*}

* Correspondence: xupeng@uestc.edu.cn; dyao@uestc.edu.cn

¹Key Laboratory for NeuroInformation of Ministry of Education, School of Life Science and Technology, University of Electronic Science and Technology of China, Chengdu 610054, China

²Center for Information in BioMedicine, University of Electronic Science and Technology of China, Chengdu 610054, China

Abstract

Resting-state functional connectivity reveals intrinsic, spontaneous networks that elucidate the functional architecture of the human brain. The default mode network (DMN) is the most important and stable intrinsic connectivity network (ICN), which involves several cognition functions, such as episodic memory and self-introspection. It has been suggested that low-frequency fluctuations in the blood oxygenation level-dependent (BOLD) signal during rest reflect the neuronal baseline activity of the brain and these low-frequency fluctuations correspond to functionally relevant resting-state networks. Several studies have revealed that the function of the brain is accomplished in certain low sub-frequency band. However, the concerned frequency bands are determined by experience, neglecting the intrinsic information of BOLD time series. In this study, we apply a full data-driven analysis, i.e., multivariate empirical mode decomposition (MEMD), to decompose resting-state fMRI data into the different sub-band DMNs, aiming to reveal the corresponding connectivity functions in separate sub-band DMN. Our results revealed that MEMD can adaptively decompose signals into intrinsic mode functions (IMFs) with the similar patterns across subjects. Furthermore, the sub-network constructed from the IMFs revealed that the different sub-band DMNs correspond to the different brain functional connectivity, inferring the possible relationships between sub-frequency band and cognitions. Owing to its data-driven merit, the proposed MEMD analysis may provide a new insight for fMRI-related studies.

Keywords: fMRI; MEMD; resting-state; default mode network; sub-frequency band

Background

The intrinsic, spontaneous low-frequency fluctuations during resting state reflected the neuronal baseline activity of the brain. The time-frequency analysis of the blood oxygenation level-dependent (BOLD) signals has drawn attention of neuroimaging investigators (Cordes et al. 2001; Salvador et al. 2008). Investigators believe that the low-frequency fluctuations may provide information about the intrinsic functional organization of the brain (Kong et al. 2013; Fox and Raichle 2007). Accumulating evidences demonstrate that resting-state baseline activity may facilitate the engagement of

brain networks necessary for responding to external stimuli (Zou et al. 2013; Smith et al. 2009).

The resting-state brain forms at least seven intrinsic connectivity networks, such as default mode network (DMN) and fronto-parietal network (FPN), which suggest the relevance for understanding the human behavior responses and cognition (Redcay et al. 2013; Fair et al. 2008). In recent years, the DMN as a critical intrinsic connectivity network has drawn a considerable attention (van den Heuvel et al. 2009; Spreng et al. 2013; Raichle et al. 2001). DMN consistently shows higher level organizations during rest than during a wide range of cognitive tasks (Pfefferbaum et al. 2011; Fox et al. 2005). It plays a leader and coordinator role in among networks (Toro et al. 2008). DMN is involved with several cognition functions like sense of internal and external environment, memory, and self-related functions (Iacoboni et al. 2004; Kompus 2011). Functional connectivity abnormal in the DMN may be relevant to some diseases, such as Alzheimer's disease (AD), epilepsy, and pain (Luo et al. 2011; Vanhaudenhuyse et al. 2009).

In BOLD signal, sub-components oscillating at different frequencies may indicate different coherence brain patterns and cognitive processes (Zhan et al. 2014). However, various literatures have shown that the low-frequency BOLD oscillation (0.01 to 0.08 Hz) is the main contributor to the brain activity (Wu et al. 2008; Fox and Raichle 2007). Wang et al. suggest that arbitrary selection of frequency band may lead to two limitations (a. caused information loss of the other frequency realms; b. mingle any physiological fluctuations with potentially specific frequencies) (Wang et al. 2014). For example, Niazy et al. proposed that lower or higher frequency BOLD signals were relevant for brain activity (Niazy et al. 2011).

Recently, several studies through predefined frequency bands have been reported to explore reciprocal connections between regions instead of between/within known brain networks (Achard et al. 2006; Salvador et al. 2007). Baria et al. discussed the different spatial distribution of four frequency bands spanning over the full BOLD bandwidth, by using the Welch spectrum estimation for all the voxels that involved in the BOLD oscillation (Baria et al. 2011). Zuo et al. specifically designed six band-pass filters that were used to separate fMRI time series into desired frequency bands (Zuo et al. 2010; Zhan et al. 2014). However, it is still unclear that how the different oscillation frequency band is correlated with the functional connectivity in the resting-state brain. Those concerned frequency bands are determined by the subject's experiences, and those subjectively based analysis may distort the intrinsic information hidden in the signal.

Thus, compared with the subjectively based analysis, the data-driven analysis is directly derived from the signal characteristics, and it may adaptively capture the hidden information in concerned signals. In the current study, we applied a fully data-driven method called multivariate empirical mode decomposition (MEMD) (Park et al. 2013) to adaptively decompose the fMRI data into the intrinsic modes with different frequency bands. The multivariate EMD, first introduced by Rehman and Mandic (2010), is a natural and generic extension of the standard EMD. The principle of EMD (Huang et al. 1998) is based on the concept of the local extrema. The original signal is modeled as a linear combination of intrinsic oscillatory modes, called intrinsic mode functions (IMFs). Unlike EMD, MEMD better aligns the corresponding to IMFs from different channels across the same frequency range which is crucial for real world applications

(Ur Rehman et al. 2010). Therefore, we will use MEMD to find the frequency-dependent sub-networks in DMN.

Methods

Subjects

Twenty-five right hand-dominant university volunteers (9 females and 16 males, aged 22.85 ± 2.48 years, range 19 to 26) were recruited in our experiment. The present study was approved by the Institution Research Ethics Board of the University of Electronic Science and Technology of China. All participants were free of medication and central nervous system abnormalities. Written informed consent was provided by each participant before any study procedure was initiated.

fMRI data acquisition

Five minutes of resting fMRI data were acquired on a 3.0-T SIEMENS MRI scanner, using an eight-channel-phased array head coil. Foam padding was used to minimize head movement. During data acquisition, participants were instructed to hold still, close eyes, and relax minds. Functional images were performed by a single-shot, gradient recalled echo-planar imaging (EPI) sequences. Sequence parameters were as follows: TR/TE/flip angle = 2000 ms / 30 ms / 90°, acquisition matrix = 64×64 , field of view (FOV) = 220×220 mm², voxel size = $3.4375 \times 3.4375 \times 4$ mm³, and thickness = 3 mm with 1-mm gap. For each participant, the brain volume comprised 32 axial slices; each functional run contained 200 image volumes.

fMRI data preprocessing

Image preprocessing was carried out using the statistical parametric mapping (SPM8, <http://www.fil.ion.ucl.ac.uk/spm>) software package implemented in the Matlab 2013a. The detailed procedures were as follows: (1) the first five volumes were discarded, (2) corrected for the temporal differences, and (3) realigned to correct head motion; the translation and rotation were checked, the images with head motion greater than 1.5 mm in the x , y , or z direction or head rotation greater than 1.5° were excluded, and six subjects were excluded in our study; (4) spatial normalization to the Montreal Neurological Institute (MNI) EPI template and resampled to 3-mm cubic voxels; (5) spatial smoothing with a 8-mm full-width at half maximum (FWHM) Gaussian kernel; (6) some literatures demonstrated that the lower (0 to 0.01Hz) or higher (0.08 to 0.25 Hz) frequency BOLD signals also have physiological significance (Baliki et al. 2014; Wang et al. 2014); thus, in order to avoid arbitrary selection of frequency band, we did temporally band-pass filtered (0 to 0.25 Hz), (7) regressing out of the six motion parameters which obtained by rigid body correction, white matter, and whole brain signals (Liu et al. 2013).

Region of interest selection and time series extraction

The DMN is an important intrinsic connectivity network and also is the most extensively studied resting-state network in the brain (Raichle and Snyder 2007). When the DMN is determined by independent component analysis or by seed-based analysis (Damoiseaux et al. 2006), it is commonly defined by low-frequency BOLD oscillations.

Given previous studies (Fox et al. 2005; Toro et al. 2008), the vMPFC, aMPFC, PCC, LPC, SFC, ITC, PHG, RSP, and cerebellar tonsils (include 13 a priori regions of interest (ROIs)) are suggested as critical regions in DMN. Therefore, we focus on these regions in our study. ROIs were defined as spheres with a radius of 6 mm. The BOLD time series was extracted from each of the 33 voxels in each ROI and then averaged across all voxels in this ROI for further analysis. The detailed information for the 13 ROIs is given in Table 1 and Figure 1.

BOLD time series processes procedure

For each participant, we first obtained the multivariate time series (13×195). Then, the MEMD method was adopted to decompose the multivariate signals into different IMF levels which have common frequency components. We used the Matlab code of MEMD which comes from (<http://www.commsp.ee.ic.ac.uk/~mandic/research/emd.htm>). Thus, a new multivariate time series ($13 \times 195 \times 6$) was obtained in every IMF level which represents a different frequency band. We calculated the functional connectivity in all IMF levels for every subject, resulting in the same number 13×13 correlation coefficients matrixes with IMF levels. The matrixes represent the strength of the functional connectivity between all 13 areas in sub-DMNs. The correlation coefficients were *z*-standardized by Fisher's *r*-to-*z* transformation to approximate a Gaussian distribution. Finally, we did one-sample *t* test $P < 0.05$ (FDR-corrected) to examine whether it was significantly on the group level, based *z*-value pairs of ROI in various IMF levels. The details about the processing scheme were shown in Figure 2.

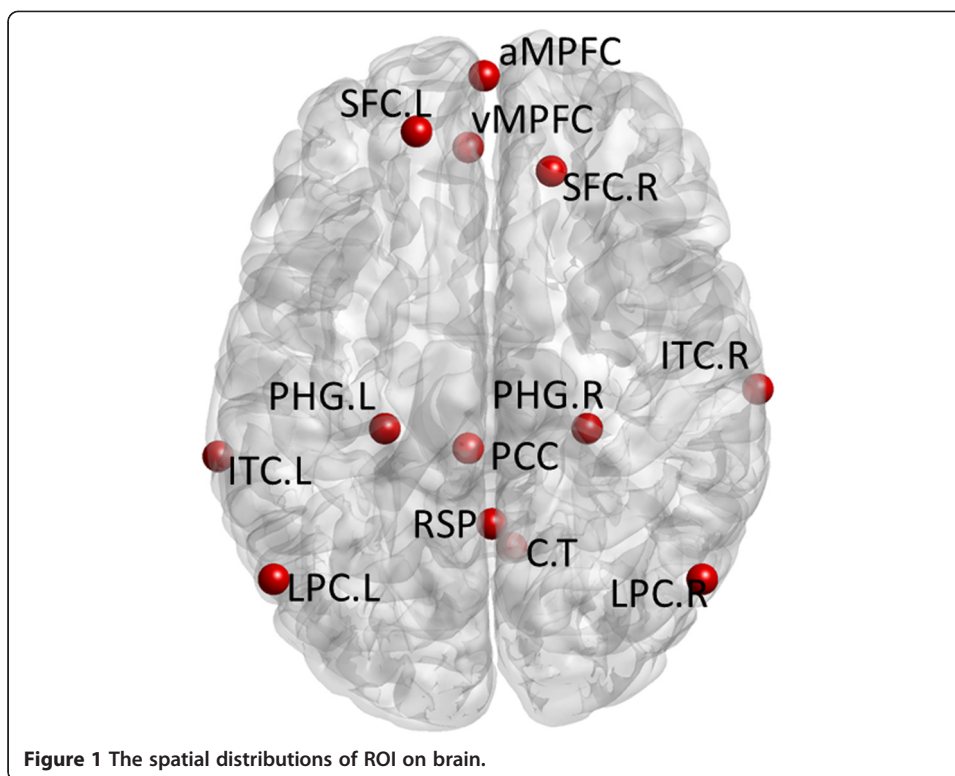
Results

IMFs of MEMD

For the 19 subjects, we found that the number of IMFs achieved by decomposing the time series of 13 ROIs which use MEMD is ranged from 8 to 10. To uniform the data, we calculated the Pearson correlation coefficients *r* between every IMF and original

Table 1 Regions of interest in DMN

Regions	Abbreviations	Coordinates (MNI)		
		<i>x</i>	<i>y</i>	<i>z</i>
Medial prefrontal cortex (ventral)	vMPFC	-4	43	-11
Medial prefrontal cortex (anterior)	aMPFC	0	61	13
Posterior cingulate cortex	PCC	-4	-33	40
Left lateral parietal cortex	LPC.L	-53	-66	41
Right lateral parietal cortex	LPC.R	55	-66	43
Left superior frontal cortex	SFC.L	-17	47	49
Right superior frontal cortex	SFC.R	17	37	49
Left inferior temporal cortex	ITC.L	-67	-35	-19
Right inferior temporal cortex	ITC.R	69	-18	-18
Left parahippocampal gyrus	PHG.L	-25	-28	-17
Right parahippocampal gyrus	PHG.R	26	-28	-17
Cerebellar tonsils	C.T	7	-58	-48
Retrosplenial	RSP	2	-52	10



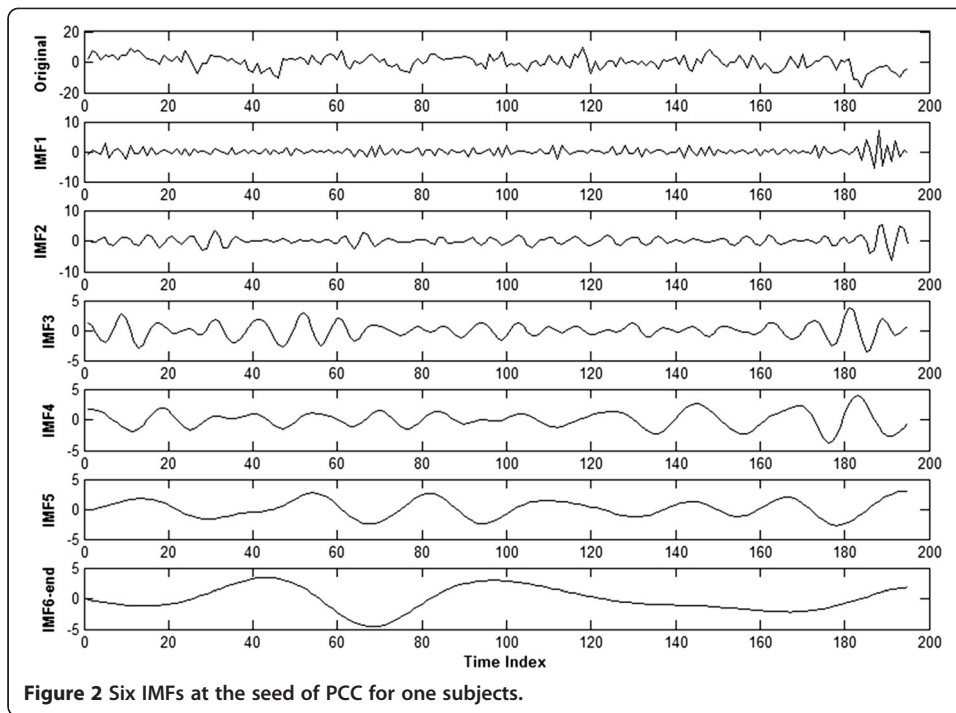
BOLD signal. We found that between the first five IMFs and original BOLD time series have high r values ($r > 0.5$). Then, we reconstructed the sixth IMF and remaining IMFs as one IMF. Thus, six IMFs were obtained for further analysis. The PCC, as a core hub region of DMN, played an important role in DMN. In this study, we only display the changes of BOLD time series at the seed of PCC. Figure 3 showed the six IMFs of BOLD time series signal of the PCC for one subject.

The center frequency band of different IMFs

Based on the decomposed IMFs for each subject, the center frequency band of IMF can be estimated using Fourier transform. Though the BOLD signal is distinct for different subjects, the center frequency band of different IMFs of every ROI in all subjects is relatively stable. Figure 4 shows the frequency distribution of one ROI (PCC) for six IMFs across all subjects. And, we found that the center frequency band is decreased from IMF1 to IMF6-end and the frequency gap of discrete mode is obvious.

Functional Connectivity of DMN in different frequency sub-bands

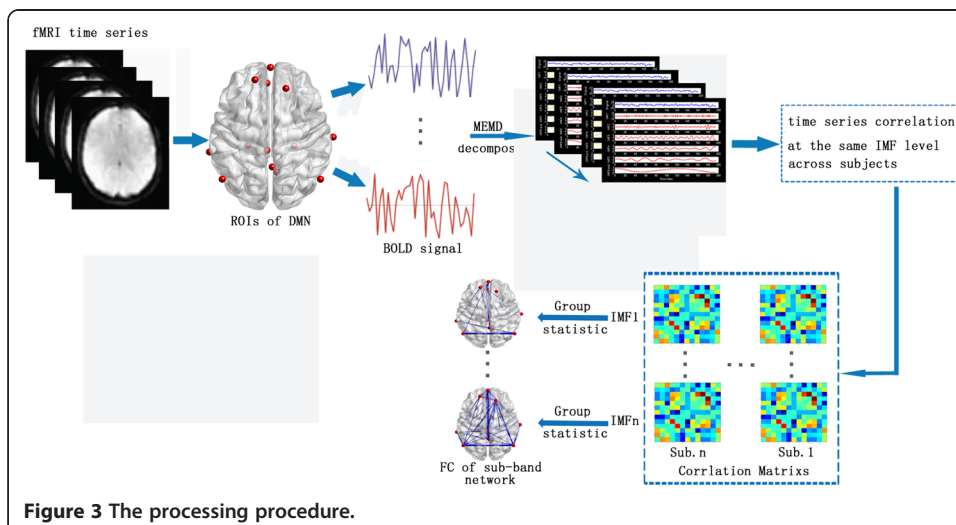
Six data-driven IMFs represent six different frequency bands of the BOLD signal. We constructed the functional connectivity networks for six IMF levels. Figure 5 clearly shows that the network topologies are obviously different for different IMFs, which may infer the different brain functions are performed in certain frequency-dependent sub-networks. Furthermore, we calculated the degree centrality of the network in each sub-band DMNs for 13 ROIs. We found that the different sub-band networks show the different degree properties that may further infer the different functions of sub-band networks.



Discussion

The main aim of the current investigation was to observe the variety of the intrinsic functional connectivity of DMN in different frequency bands, using a full data-driven method MEMD. Our findings showed that the MEMD is an effective method to adaptively decompose the BOLD signals into different frequency bands according to the time series nature characteristics. And, the functional connectivity networks were significant distinct at the different frequency bands, especially in the ultra-low-frequency range (0 to 0.08) which the network has a high-efficiency system. Our results may provide a new insight into the frequency specificity of functional connectivity in the DMN.

There is a large body of literature suggesting that the frequency-specific characteristic exists in the resting-state fMRI signals within multiple functional brain networks (Wu



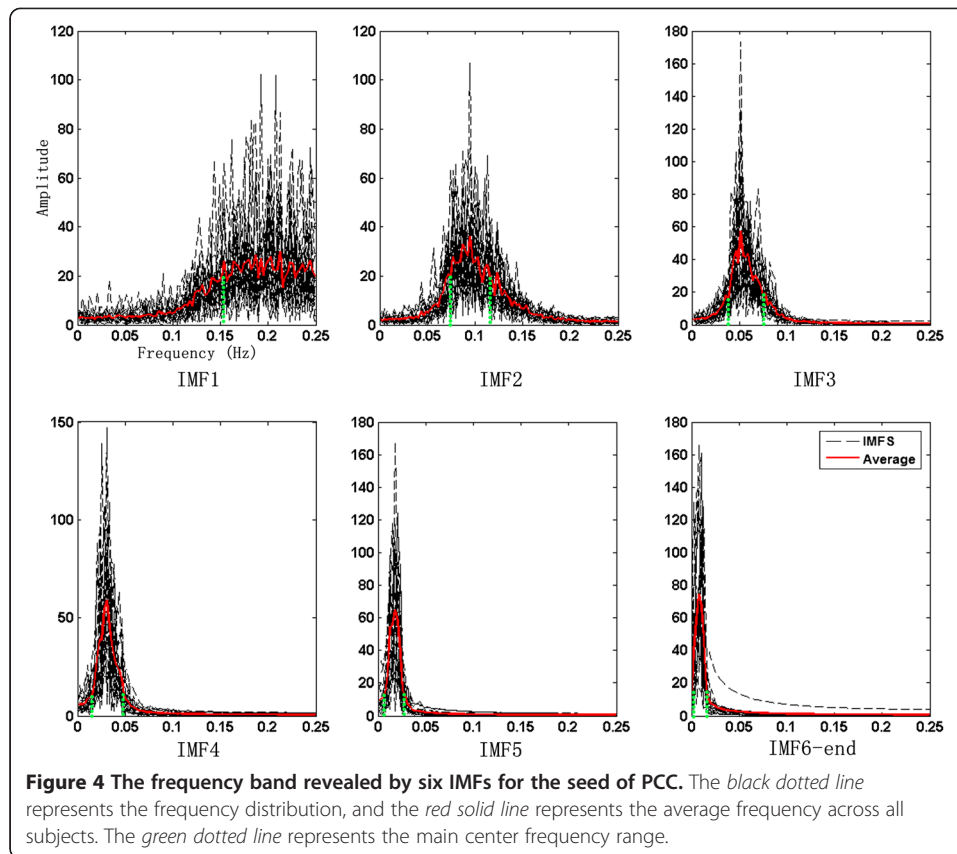
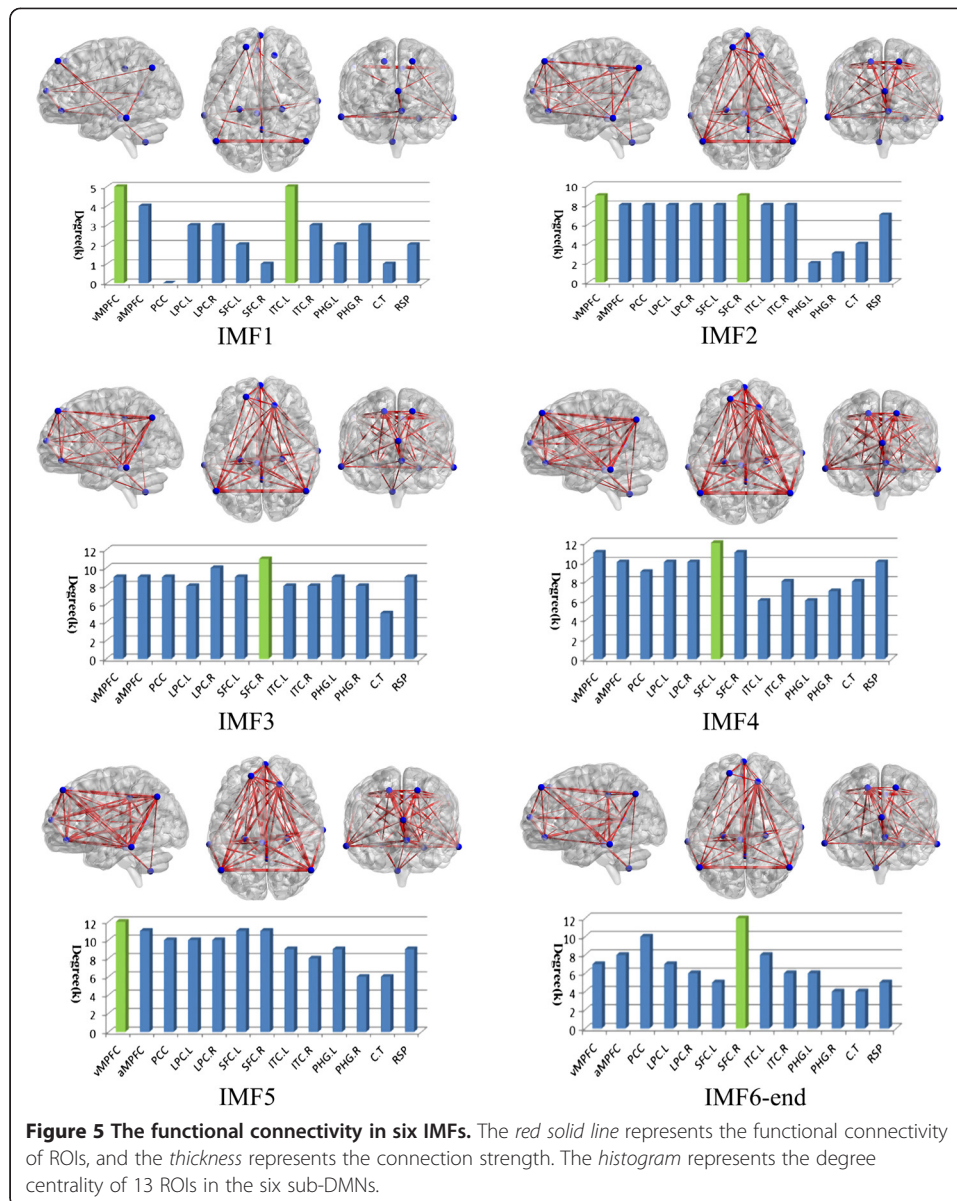


Figure 4 The frequency band revealed by six IMFs for the seed of PCC. The black dotted line represents the frequency distribution, and the red solid line represents the average frequency across all subjects. The green dotted line represents the main center frequency range.

et al. 2008; Zuo et al. 2010). Studies suggest that in BOLD signal, the sub-component fluctuation at different frequency bands may predict different coherence brain patterns and cognitive processes (Zuo et al. 2010; Zhan et al. 2014). The functional connectivity at the low-frequency oscillations (0.01 to 0.08 Hz) was suggested a major contributor to understanding of human cognition and behavior (Fox and Raichle 2007; Zhu et al. 2011).

In recent studies, investigators suggested that subdivided frequency bands, including slow-5 (0.01 to 0.027 Hz), slow-4 (0.027 to 0.073 Hz), slow-3 (0.073 to 0.198 Hz), and slow-2 (0.198 to 0.25 Hz), may have different meanings (Zuo et al. 2010); Baliki et al. found that multiple DMN regions exhibited increased high-frequency (0.12 to 0.20 Hz) oscillations, conjoined with decreased phase locking with parietal regions involved in processing attention (Baliki et al. 2014).

In the current study, we found that the MEMD decomposed the BOLD time series of DMN into different IMFs across subjects, with the specified center frequency band for each IMF. From IMF1 to IMF6-end, six subdivided frequency bands were achieved by MEMD, including the mainly center frequency bands IMF1 (0.15 to 0.25 Hz), IMF2 (0.08 to 0.15 Hz), IMF3 (0.03 to 0.08 Hz), IMF4 (0.02 to 0.05 Hz), IMF5 (0.01 to 0.03 Hz), and IMF6-end (0 to 0.02 Hz), respectively. Previous studies predefined several dependent frequency bands for time-frequency analysis (Salvador et al. 2008; Buzsaki and Draguhn 2004; Zuo et al. 2010). However, we found the center frequency bands are not completely independent, where there are interactive which implied the signal intrinsic information, especially in IMF3 to IMF6-end levels. The frequency bands overlapped may indicate that dynamic changes in DMN at resting-state functional connectivity (Chang and Glover 2010).



In the IMF1 and IMF2 levels, the frequency bands are mainly distributed at high-frequency ranges 0.15 to 0.25 and 0.08 to 0.15 Hz. We found that in the IMF1 level, the functional connectivity of the sub-network is relatively weaker compared to the rest five sub-networks. Furthermore, we also found the core hub PCC of DMN was in the disconnected state. A previous study found that the 0.198- to 0.25-Hz band rarely correlated with the alpha rhythm power, even in the uncorrected significance $P < 0.001$ (Zhan et al. 2014), whereas the functional connectivity of the network is stronger in the IMF2 level. Several studies have shown that the patients with chronic pain had enhanced 0.12- to 0.25-Hz fluctuations and disturbed connectivity in their affective pain matrix (Malinen et al. 2010; Wu et al. 2008).

From IMF3 to IMF6-end levels, the main sub-frequency bands are 0.03 to 0.08, 0.02 to 0.05, 0.01 to 0.03, and 0 to 0.02 Hz, respectively. Previous studies have suggested that these low-frequency oscillations are major contributors to the correlation at resting

state (Cordes et al. 2001; Zuo et al. 2010; Fox and Raichle 2007). In addition to the IMF6-end levels network, we also found the corresponding four low-frequency band networks shown the increased function connectivity when the frequency is gradually decreased. Moreover, in different IMF levels, the most hub region is altered; for example, the aMPFC and right SFC have a highest degree centrality in the IMF2 level, whereas the right SFC has a highest degree centrality in the IMF3 level. These may indicate that in different frequency bands, the hub region is dynamic change in DMN.

The MPFC, PCC, and SFC are the core hub regions of DMN (Raichle et al. 2001). In our study, the degree centrality of vMPFC is kept relatively high in all sub-band DMNs, being largest in IMF1, IMF2, and IMF5 networks. This is consistent with previous studies demonstrating that vMPFC is playing a critical role in DMN. The medial prefrontal cortex (MPFC) has been proved to be associated with several functions including the internal “narrative” (Fair et al. 2008), the “autobiographical” self (Gusnard et al. 2001; Buckner and Carroll 2007), “stimulus independent thought” (Mason et al. 2007), “mentalizing,” and recently revealed “self-projection” (Frith and Frith 2003). And, we also found the PCC and SFC in the low-frequency bands have a high-degree centrality. A recent study (Dziobek et al. 2011; Cui et al. 2012) about the role of frontal cortex in empathy demonstrates that SFC is associated with the theory of mind.

In addition, the functional connectivity of the left lateral parietal cortex and the right lateral parietal cortex always exists and the connection strength is almost kept consistently high across the different sub-frequency networks. The lateral parietal area has function to differentiate and attend spatial locations (Davidson et al. 2008). LPC is important in the attentional mechanisms preceding the choice of saccade target rather than in the intention to generate the saccade itself (Goldberg et al. 2006).

Several limitations should be noted in this study. First of all, our sample size was relatively small and the age range was narrow. Larger, independent, and multi-center datasets will be necessary to improve our findings. Second, in our study, we only concerned the healthy young participants. As we known, the functional connectivity of DMN related to several high-order cognition and diseases, such as AD, pain, and depression (Kornelsen et al. 2013; Luo et al. 2011; Yao et al. 2013). Third, the current work is focused on the resting-state fMRI. As for task-related fMRI, the related cognition process can also be assumed to be performed in different frequency bands. Therefore, MEMD can also be employed to decompose task fMRI into sub-frequency bands. In our future work, we will further probe the analysis of task fMRI utilizing MEMD, which may provide the new insights for task fMRI. Finally, the complex network as a tool for exploring the human brain has attracted considerable attention (Lee et al. 2013; Sporns 2014). Besides the degree centrality concerned in this study, more other brain network measures like betweenness centrality, eigenvector centrality, should be considered for deepening our understanding of the DMN in different frequency bands.

Conclusions

In summary, this study used a full data-driven method to adaptively decompose BOLD signals into different bands based on the inherent characteristics of signal, which may provide more natural sub-frequency bands for fMRI analysis. Further analysis demonstrates that sub-network constructed from the IMFs revealed that the different sub-

band DMNs corresponds to the different brain functions, inferring the possible relationships between frequency band and cognitions. Our results imply that brain functions of DMN may be frequency specified. Due to its data-driven merit, the proposed MEMD analysis may provide a new insight for fMRI-related studies.

Abbreviations

BOLD: blood oxygenation level-dependent; DMN: default mode network; ICN: intrinsic connectivity network; MEMD: multivariate empirical mode decomposition; IMFs: intrinsic mode functions; Rs fMRI: resting-state functional connectivity MRI; ROI: region of interest; FPN: fronto-parietal network; AD: Alzheimer's disease.

Competing interests

The authors declare that they have no competing interests.

Authors' contributions

PX, TZ, and LG conceived and designed the experiments. LG, RC, and RZ performed the experiment. TZ and LG analyzed the data. TZ, LG, and RC contributed reagents/materials/analysis tools. TZ, PX, and DY wrote the paper. All authors read and approved the final manuscript.

Acknowledgment

This work was supported in part by grants from the 973 program 2011CB707803, the National Natural Science Foundation of China (no. 61175117, no. 81330032, no. 31200857, and no. 31100745), the program for New Century Excellent Talents in University (no. NCET-12-0089), the 863 project 2012AA011601, and the National Science and Technology Pillar Program 2012BAI16B02.

Received: 4 August 2014 Accepted: 22 December 2014

Published online: 16 January 2015

References

- Achard S, Salvador R, Whitcher B, Suckling J, Bullmore E (2006) A resilient, low-frequency, small-world human brain functional network with highly connected association cortical hubs. *J Neurosci* 26(1):63–72, doi:10.1523/JNEUROSCI.3874-05.2006
- Baliki MN, Mansour AR, Baria AT, Apkarian AV (2014) Functional reorganization of the default mode network across chronic pain conditions. *PLoS one* 9(9):e106133, doi:10.1371/journal.pone.0106133
- Baria AT, Baliki MN, Parrish T, Apkarian AV (2011) Anatomical and functional assemblies of brain BOLD oscillations. *J Neurosci* 31(21):7910–7919, doi:10.1523/JNEUROSCI.1296-11.2011
- Buckner RL, Carroll DC (2007) Self-projection and the brain. *Trends in cognitive sciences* 11(2):49–57, doi:10.1016/j.tics.2006.11.004
- Buzsaki G, Draguhn A (2004) Neuronal oscillations in cortical networks. *Science* 304(5679):1926–1929, doi:10.1126/science.1099745
- Chang C, Glover GH (2010) Time-frequency dynamics of resting-state brain connectivity measured with fMRI. *NeuroImage* 50(1):81–98, doi:10.1016/j.neuroimage.2009.12.011
- Cordes D, Haughton VM, Arfanakis K, Carew JD, Turski PA, Moritz CH et al (2001) Frequencies contributing to functional connectivity in the cerebral cortex in "resting-state" data. *AJNR American journal of neuroradiology* 22(7):1326–1333
- Cui X, Bryant DM, Reiss AL (2012) NIRS-based hyperscanning reveals increased interpersonal coherence in superior frontal cortex during cooperation. *NeuroImage* 59(3):2430–2437, doi:10.1016/j.neuroimage.2011.09.003
- Damoiseaux JS, Rombouts SA, Barkhof F, Scheltens P, Stam CJ, Smith SM et al (2006) Consistent resting-state networks across healthy subjects. *Proc Natl Acad Sci U S A* 103(37):13848–13853, doi:10.1073/pnas.0601417103
- Davidson PS, Anaki D, Ciaramelli E, Cohn M, Kim AS, Murphy KJ et al (2008) Does lateral parietal cortex support episodic memory? Evidence from focal lesion patients. *Neuropsychologia* 46(7):1743–1755
- Dziobek I, Preissler S, Grodzanovic Z, Heuser I, Heekeren HR, Roepke S (2011) Neuronal correlates of altered empathy and social cognition in borderline personality disorder. *NeuroImage* 57(2):539–548, doi:10.1016/j.neuroimage.2011.05.005
- Fair DA, Cohen AL, Dosenbach NU, Church JA, Miezin FM, Barch DM et al (2008) The maturing architecture of the brain's default network. *Proc Natl Acad Sci U S A* 105(10):4028–4032, doi:10.1073/pnas.0800376105
- Fox MD, Raichle ME (2007) Spontaneous fluctuations in brain activity observed with functional magnetic resonance imaging. *Nat Rev Neurosci* 8(9):700–711, doi:10.1038/Nrn2201
- Fox MD, Snyder AZ, Vincent JL, Corbetta M, Van Essen DC, Raichle ME (2005) The human brain is intrinsically organized into dynamic, anticorrelated functional networks. *Proc Natl Acad Sci U S A* 102(27):9673–9678, doi:10.1073/pnas.0504136102
- Frith CD (2003) Development and neurophysiology of mentalizing. *Philos Trans R Soc Lond B Biol Sci* 358(1431):459–473, doi:10.1098/rstb.2002.1218
- Goldberg ME, Bissley JW, Powell KD, Gottlieb J (2006) Saccades, salience and attention: the role of the lateral intraparietal area in visual behavior. *Prog Brain Res* 155:157–175
- Gusnard DA, Akbudak E, Shulman GL, Raichle ME (2001) Medial prefrontal cortex and self-referential mental activity: relation to a default mode of brain function. *Proc Natl Acad Sci U S A* 98(7):4259–4264, doi:10.1073/pnas.071043098
- Huang NE, Shen Z, Long SR, Wu MC, Shih HH, Zheng Q et al (1998) The empirical mode decomposition and the Hilbert spectrum for nonlinear and non-stationary time series analysis. *Proc R Soc Lond A Math Phys Eng Sci* 454(1971):903–995
- Iacoboni M, Lieberman MD, Knowlton BJ, Molnar-Szakacs I, Moritz M, Throop CJ et al (2004) Watching social interactions produces dorsomedial prefrontal and medial parietal BOLD fMRI signal increases compared to a resting baseline. *NeuroImage* 21(3):1167–1173, doi:10.1016/j.neuroimage.2003.11.013
- Kompus K (2011) Default mode network gates the retrieval of task-irrelevant incidental memories. *Neurosci Lett* 487(3):318–321, doi:10.1016/j.neulet.2010.10.047

- Kong J, Jensen K, Loiotile R, Cheetham A, Wey HY, Tan Y et al (2013) Functional connectivity of the frontoparietal network predicts cognitive modulation of pain. *Pain* 154(3):459–467, doi:10.1016/j.pain.2012.12.004
- Kornelsen J, Sbotto-Frankensteen U, Mclver T, Gervai P, Wacnik P, Berrington N et al (2013) Default mode network functional connectivity altered in failed back surgery syndrome. *J Pain* 14(5):483–491, doi:10.1016/j.jpain.2012.12.018
- Lee MH, Smyser CD, Shimony JS (2013) Resting-state fMRI: a review of methods and clinical applications. *AJNR Am J Neuroradiol* 34(10):1866–1872, doi:10.3174/ajnr.A3263
- Liu F, Wee CY, Chen H, Shen D (2013) Inter-modality relationship constrained multi-modality multi-task feature selection for Alzheimer's Disease and mild cognitive impairment identification. *NeuroImage* 84C:466–475, doi:10.1016/j.neuroimage.2013.09.015
- Luo C, Li Q, Lai Y, Xia Y, Qin Y, Liao W et al (2011) Altered functional connectivity in default mode network in absence epilepsy: a resting-state fMRI study. *Hum Brain Mapp* 32(3):438–449
- Malinen S, Vartiainen N, Hlushchuk Y, Koskinen M, Ramkumar P, Forss N et al (2010) Aberrant temporal and spatial brain activity during rest in patients with chronic pain. *Proc Natl Acad Sci U S A* 107(14):6493–6497, doi:10.1073/pnas.1001504107
- Mason MF, Norton MI, Van Horn JD, Wegner DM, Grafton ST, Macrae CN (2007) Wandering minds: the default network and stimulus-independent thought. *Science* 315(5810):393–395, doi:10.1126/science.1131295
- Niazy RK, Xie JY, Miller K, Beckmann CF, Smith SM (2011) Spectral characteristics of resting state networks. Slow brain oscillations of sleep. *Resting State and Vigilance* 193:259–276, doi:10.1016/B978-0-444-53839-0.00017-X
- Park C, Looney D, Naveed ur R, Ahrabian A, Mandic DP (2013) Classification of motor imagery BCI using multivariate empirical mode decomposition. *IEEE Trans Neural Syst Rehabil Eng* 21(1):10–22, doi:10.1109/TNSRE.2012.2229296
- Pfefferbaum A, Chanraud S, Pitel AL, Muller-Oehring E, Shankaranarayanan A, Alsup DC et al (2011) Cerebral blood flow in posterior cortical nodes of the default mode network decreases with task engagement but remains higher than in most brain regions. *Cereb cortex* 21(1):233–244, doi:10.1093/cercor/bhq090
- Raichle ME, MacLeod AM, Snyder AZ, Powers WJ, Gusnard DA, Shulman GL (2001) A default mode of brain function. *Proc Natl Acad Sci U S A* 98(2):676–682, doi:10.1073/pnas.98.2.676
- Raichle ME, Snyder AZ (2007) A default mode of brain function: a brief history of an evolving idea. *NeuroImage* 37(4):1083–1090, discussion 1097–1089 doi:10.1016/j.neuroimage.2007.02.041
- Redcay E, Moran JM, Mavros PL, Tager-Flusberg H, Gabrieli JD, Whitfield-Gabrieli S (2013) Intrinsic functional network organization in high-functioning adolescents with autism spectrum disorder. *Front human neurosci* 7:573, doi:10.3389/fnhum.2013.00573
- Rehman N, Mandic D (2010) Multivariate empirical mode decomposition. *R Soc Lond Proc A* 466:1291–1302
- Salvador R, Martinez A, Pomarol-Clotet E, Gomar J, Vila F, Sarro S et al (2008) A simple view of the brain through a frequency-specific functional connectivity measure. *NeuroImage* 39(1):279–289, doi:10.1016/j.neuroimage.2007.08.018
- Salvador R, Martinez A, Pomarol-Clotet E, Sarro S, Suckling J, Bullmore E (2007) Frequency based mutual information measures between clusters of brain regions in functional magnetic resonance imaging. *NeuroImage* 35(1):83–88, doi:10.1016/j.neuroimage.2006.12.001
- Smith SM, Fox PT, Miller KL, Glahn DC, Fox PM, Mackay CE et al (2009) Correspondence of the brain's functional architecture during activation and rest. *Proc Natl Acad Sci U S A* 106(31):13040–13045, doi:10.1073/pnas.0905267106
- Sporns O (2014) Contributions and challenges for network models in cognitive neuroscience. *Nat Neurosci* 17(5):652–660, doi:10.1038/nm.3690
- Spreng RN, Sepulcre J, Turner GR, Stevens WD, Schacter DL (2013) Intrinsic architecture underlying the relations among the default, dorsal attention, and frontoparietal control networks of the human brain. *J Cogn Neurosci* 25(1):74–86, doi:10.1162/jocn_a_00281
- Toro R, Fox PT, Paus T (2008) Functional coactivation map of the human brain. *Cereb cortex* 18(11):2553–2559, doi:10.1093/cercor/bhn014
- Ur Rehman N, Xia Y, Mandic DP (2010) Application of multivariate empirical mode decomposition for seizure detection in EEG signals. *Conf Proc IEEE Eng Med Biol Soc* 2010:1650–1653, doi:10.1109/IEMBS.2010.5626665
- van den Heuvel MP, Mandl RC, Kahn RS, Hulshoff Pol HE (2009) Functionally linked resting-state networks reflect the underlying structural connectivity architecture of the human brain. *Hum Brain Mapp* 30(10):3127–3141, doi:10.1002/hbm.20737
- Vanhau denhuysse A, Noirhomme Q, Tshibanda LJ-F, Bruno M-A, Boveroux P, Schnakers C et al (2009) Default network connectivity reflects the level of consciousness in non-communicative brain-damaged patients. *Brain* 133:161
- Wang Z, Zhang Z, Liao W, Xu Q, Zhang J, Lu W et al (2014) Frequency-dependent amplitude alterations of resting-state spontaneous fluctuations in idiopathic generalized epilepsy. *Epilepsy Res* 108(5):853–860, doi:10.1016/j.eplepsyres.2014.03.003
- Wu CW, Gu H, Lu H, Stein EA, Chen JH, Yang Y (2008) Frequency specificity of functional connectivity in brain networks. *NeuroImage* 42(3):1047–1055, doi:10.1016/j.neuroimage.2008.05.035
- Yao H, Liu Y, Zhou B, Zhang Z, An N, Wang P et al (2013) Decreased functional connectivity of the amygdala in Alzheimer's disease revealed by resting-state fMRI. *Eur J Radiol* 82(9):1531–1538, doi:10.1016/j.ejrad.2013.03.019
- Zhan Z, Xu L, Zuo T, Xie D, Zhang J, Yao L et al (2014) The contribution of different frequency bands of fMRI data to the correlation with EEG alpha rhythm. *Brain research* 1543:235–243, doi:10.1016/j.brainres.2013.11.016
- Zhu Q, Zhang JD, Luo YLL, Dilks DD, Liu J (2011) Resting-state neural activity across face-selective cortical regions is behaviorally relevant. *J Neurosci* 31(28):10323–10330, doi:10.1523/Jneurosci.0873-11.2011
- Zou Q, Ross TJ, Gu H, Geng X, Zuo XN, Hong LE et al (2013) Intrinsic resting-state activity predicts working memory brain activation and behavioral performance. *Hum Brain Mapp* 34(12):3204–3215, doi:10.1002/hbm.22136
- Zuo XN, Di Martino A, Kelly C, Shehzad ZE, Gee DG, Klein DF et al (2010) The oscillating brain: complex and reliable. *NeuroImage* 49(2):1432–1445, doi:10.1016/j.neuroimage.2009.09.037